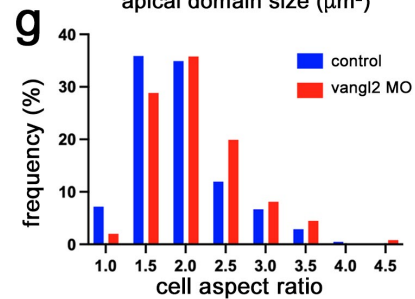
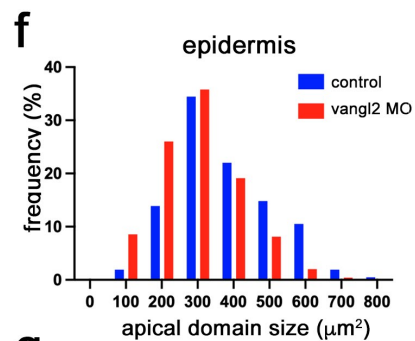
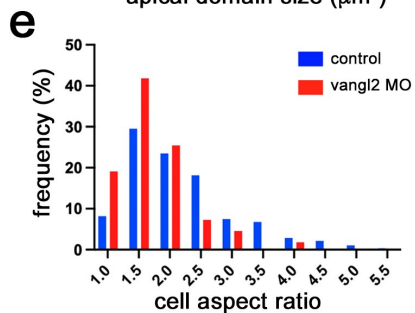
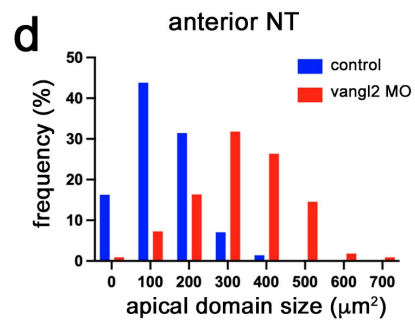
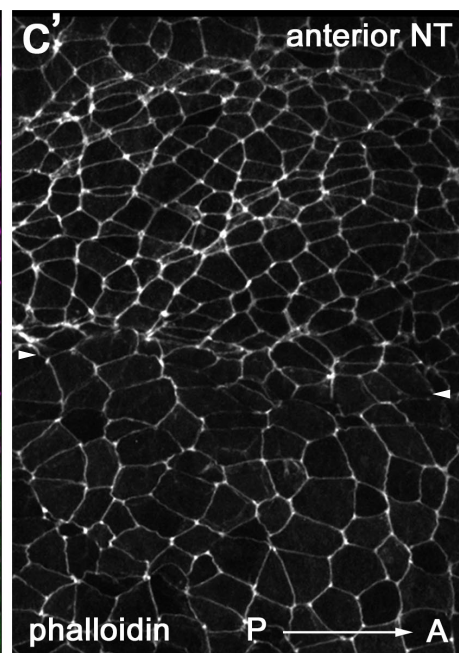
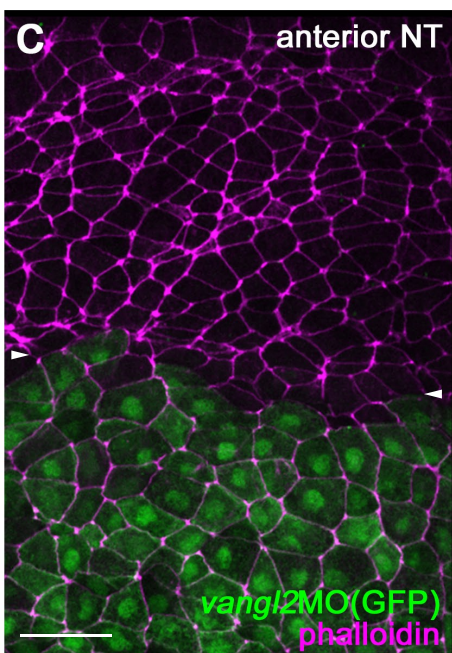
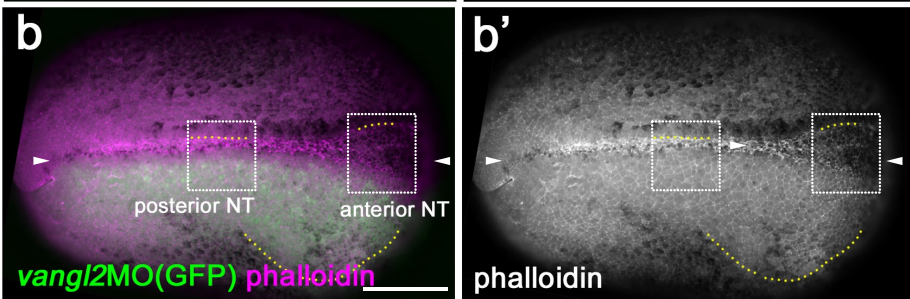
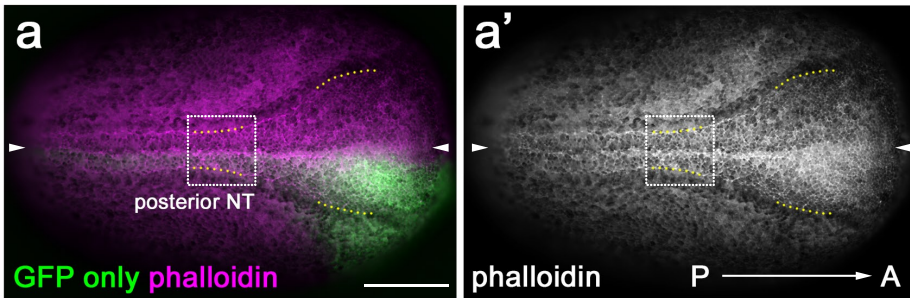


Mechanical control of neural plate folding by apical domain alteration

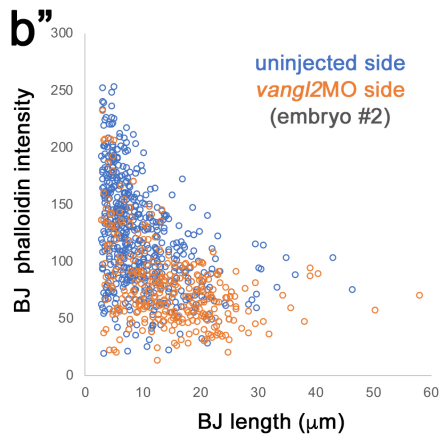
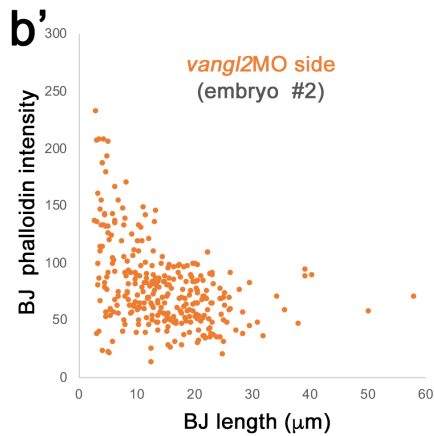
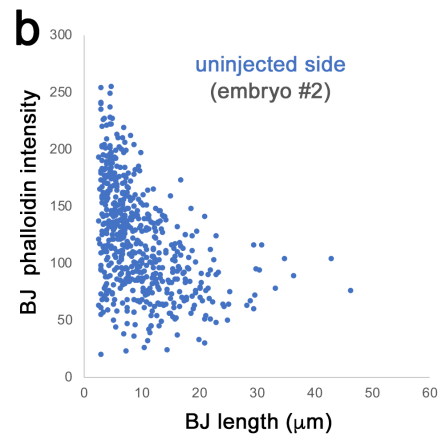
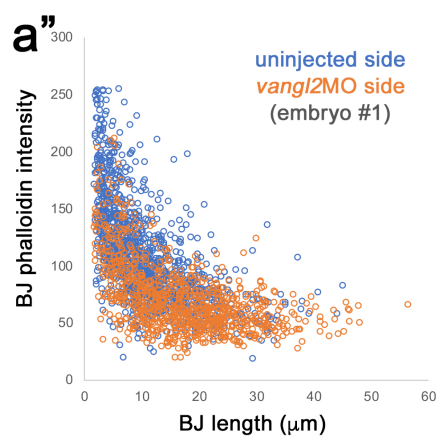
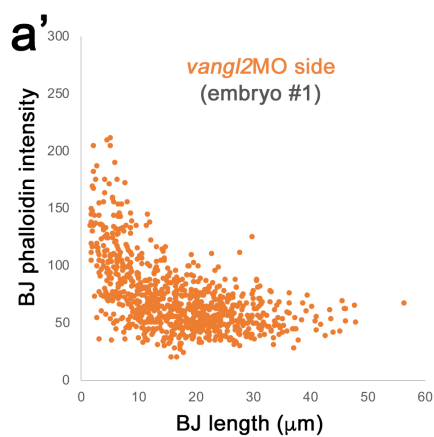
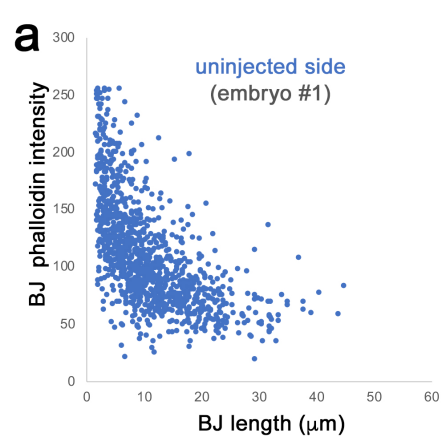
Miho Matsuda ¹, Jan Rozman ², Sassan Ostvar ³, Karen E. Kasza ³ and Sergei Y. Sokol ¹

Supplementary information: Figures S1-S11, Table S1, Movies 1-5.



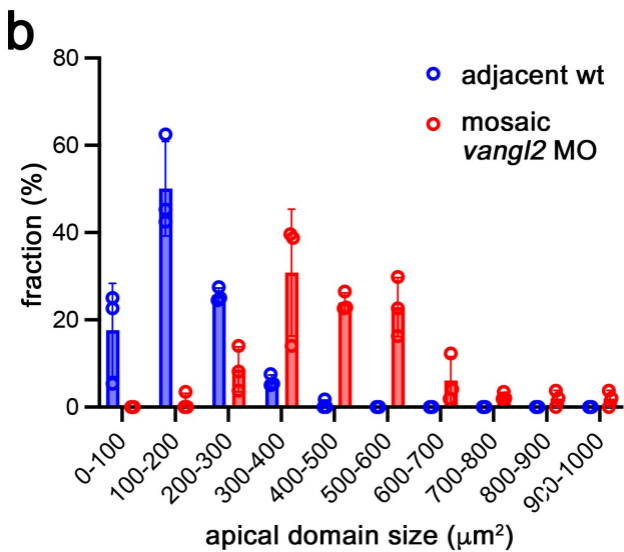
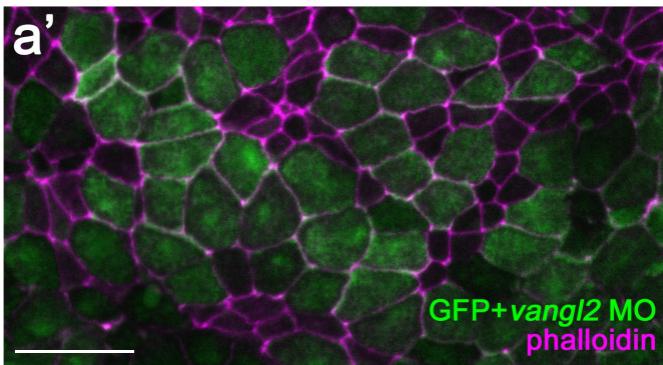
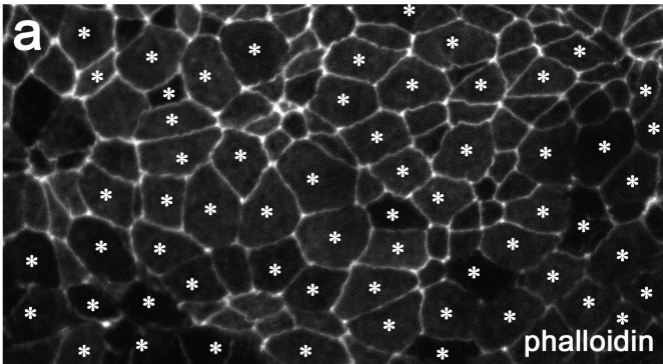
Supplementary Figure 1. PCP-dependent cell heterogeneity in the anterior and posterior neural plate.

(a-b') Representative images of injected embryos. GFP RNA and *vangl2* MO or control GFP RNA was injected into one dorsal blastomere of 4-cell stage embryos. Embryos at stage 15-16 were stained with phalloidin. The approximate locations of posterior and anterior NP images in Figs. 2a-b' and S1c-c' and are indicated in white boxes. The midline is indicated by white arrowheads. (c, c') *vangl2* knockdown increased apical domain size and decreased cell aspect ratio in the anterior neural plate. Scale bars are 100 μm in a, b and 50 μm in c. Experiments were repeated three times. (d) Comparison of apical domain size in *vangl2* MO-injected and control cells. See Methods. n=283 cells for control. N=110 cells for *vangl2* MO. (e) Cell aspect ratio for cells in c. (f) Apical domain size in the *vangl2* MO-injected and control epidermis. Note that epidermis in *vangl2* MO has smaller apical domains than control epidermis. (g) Cell aspect ratio in the *vangl2* MO injected and control epidermal cells. n=209, for control cells from 6 embryos. n=246, for *vangl2* MO containing cells from 9 embryos. Experiments were repeated three times. Statistical significance was assessed using the Kolmogorov-Smirnov test. $p < 0.0000000001$ (d). $p = 0.000000939$ (e). $p = 0.000002587$ (f). $p = 0.0027$ (g).



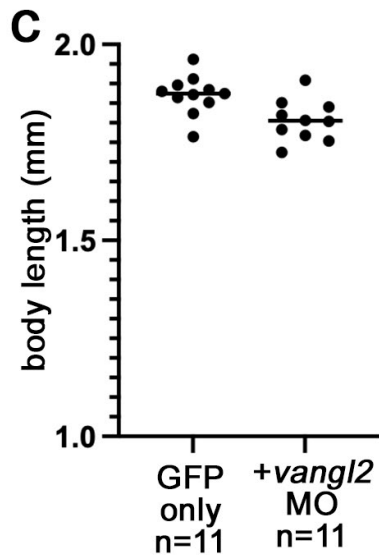
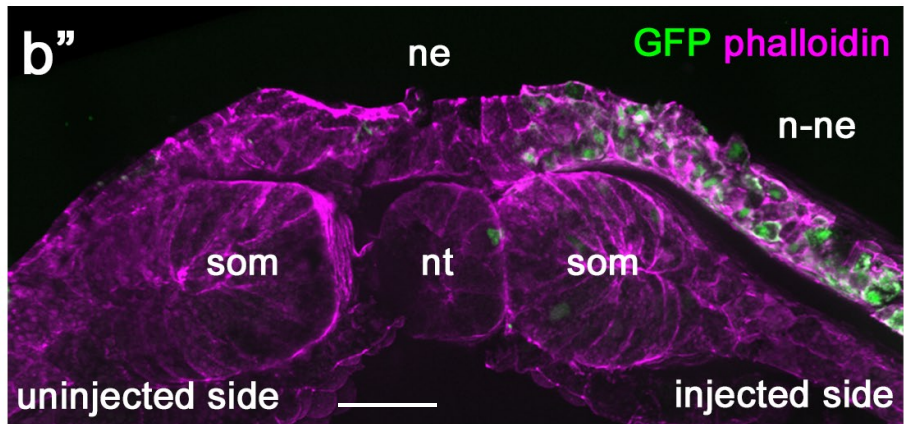
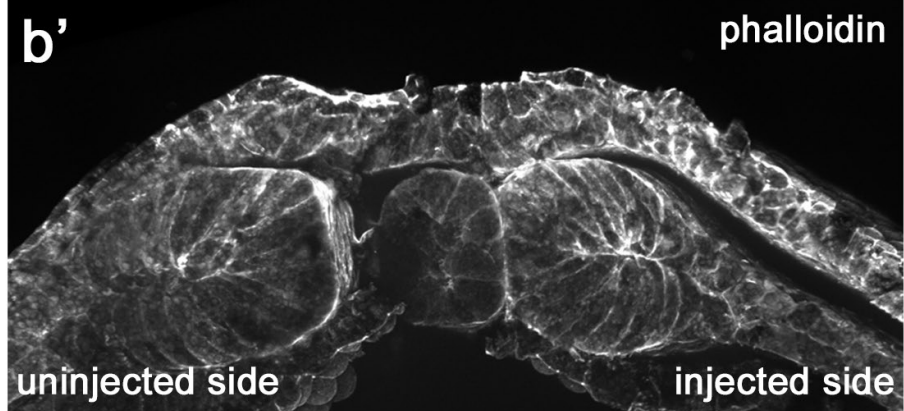
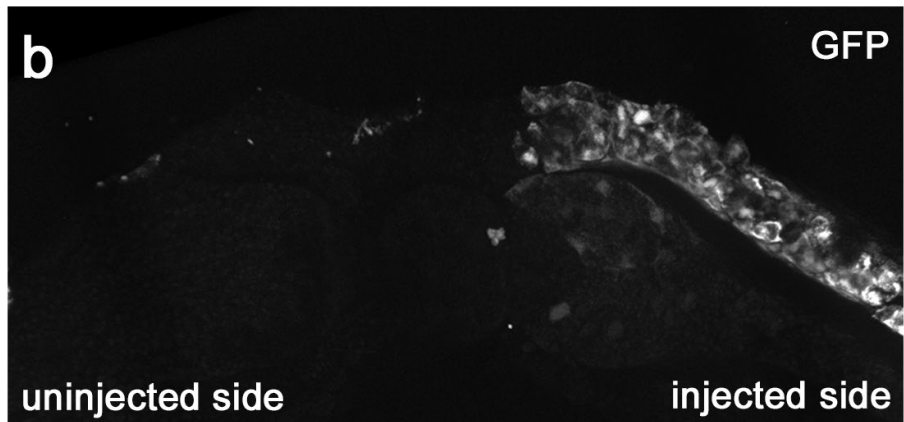
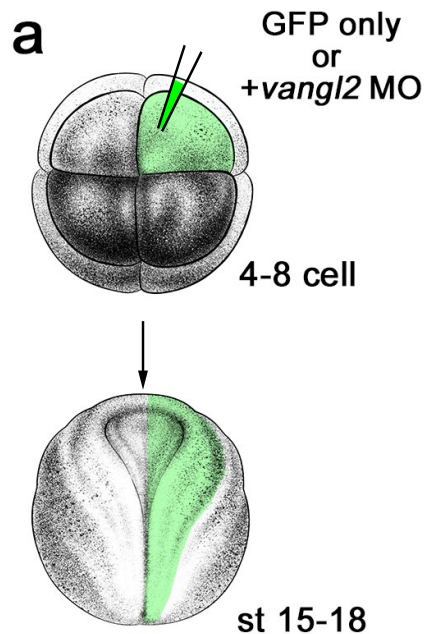
Supplementary Figure 2. Quantification of bicellular junction length and phalloidin intensity in Vangl2-depleted and wild-type neuroepithelial cells.

(a-b'') Quantification of bicellular junction (BJ) length and the average relative phalloidin intensity in the area bordering the anterior and the posterior regions of NP. Two different embryos are shown in a and b. The uninjected control side (blue in a, a'', b, b''). *vangl2* MO-injected side (orange in a', a'', b', b''). Individual dots represent individual BJs. n=1121 cells for uninjected in a, a''. n=856 cells for *vangl2* MO in a', a''. n=571 cells for uninjected in b, b'', n=307 cells for *vangl2* MO in b', b''. BJs were used for quantification to avoid the complexity of tricellular junction regulation.



Supplementary Figure 3. Effects of Vangl2 depletion on apical domain size.

Embryos were injected at the 8-16 cell stage with *vangl2* MO to achieve mosaic depletion. (a) Representative image of phalloidin-stained anterior neuroectoderm with mosaic *vangl2* depleted cells (asterisks in a, green in a'). GFP was co-injected with *vangl2* MO as a tracer. (b) Quantification of apical domain size in mosaic *vangl2* MO cells (red) and the adjacent wild-type control cells (blue). n=162 for *vangl2* MO cells and n=151 for adjacent wild-type cells from three embryos. som: somite, nt: notochord, ne: neuroectoderm, n-ne: non-neuroectoderm. The Kolmogorov-Smirnov test. $p < 0.0000000001$. Scale bar: 20 μm .



Supplementary Figure 4. Targeting of neuroectoderm by microinjection and the quantification of the body length in mosaic *Vangl2* morphants.

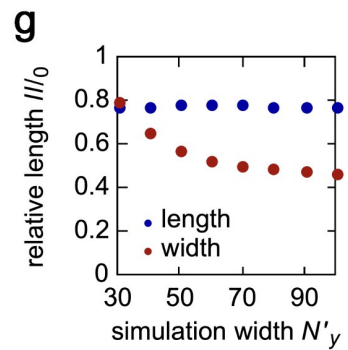
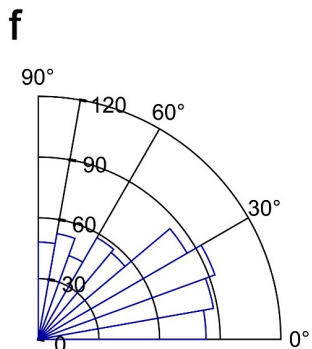
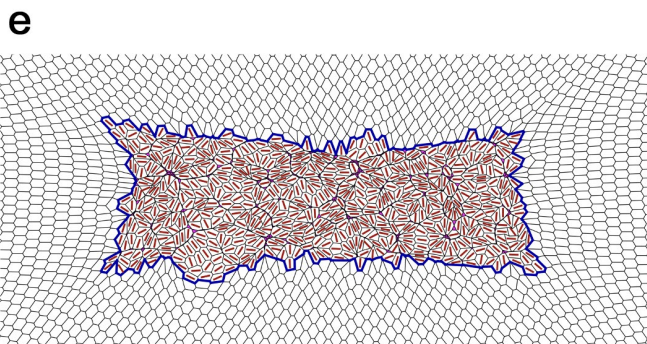
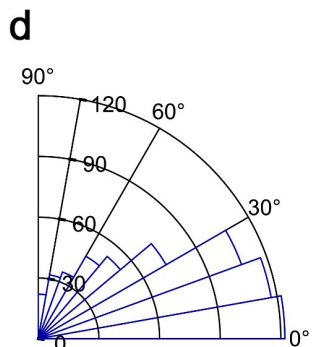
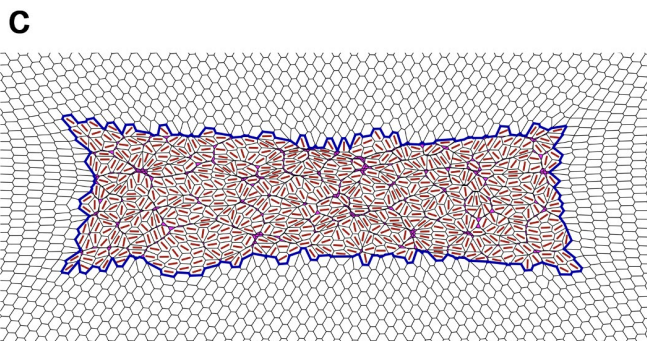
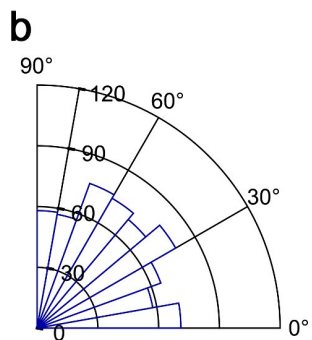
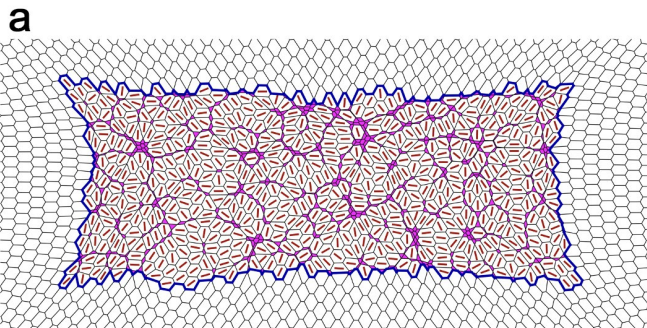
(a) Schematics of the injection experiments. Adapted from *Xenopus* illustrations ©

Natalya Zahn (2022), Xenbase (www.xenbase.org RRID:SCR_003280)¹. (b-b’)

Representative cross-section of phalloidin-stained stage 15 embryo (dorsal region) that was injected in a dorsal animal blastomere at the 4-8-cell stage with 50 pg of GFP RNA as a lineage tracer. GFP fluorescence is imaged directly after cryosectioning. b and b’, separate channels, b”, merged channels. Experiments were repeated three times. Scale

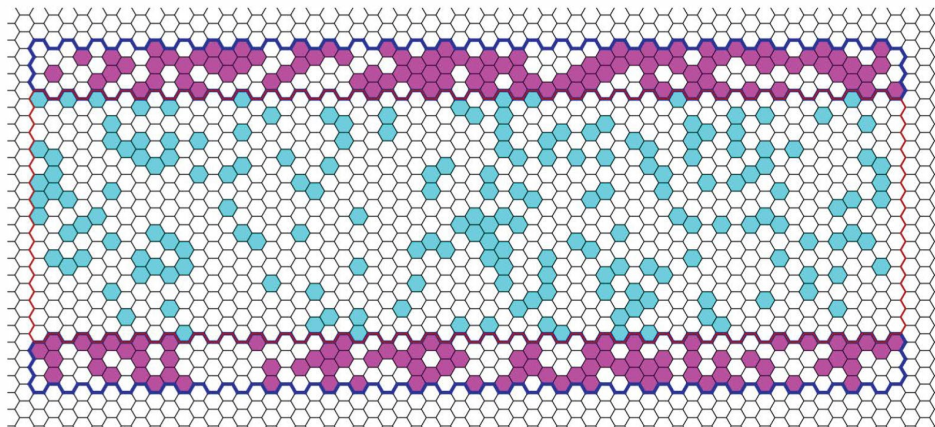
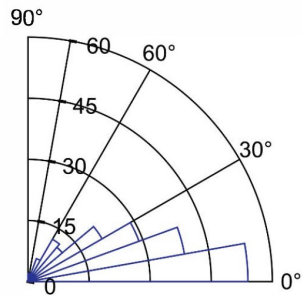
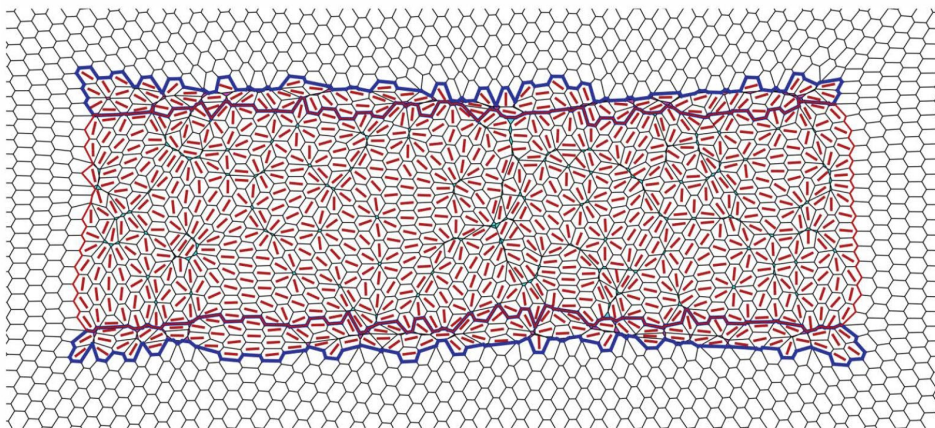
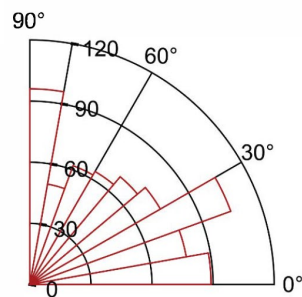
bar: 50 μ m. (c) Quantification of the body length of mosaic *vangl2* morphants at stages 16-17. n=11, for control GFP expressing embryos. n=11, for *vangl2* MO+GFP embryos.

The Student’s t-test. Two-sided. p=0.0089.



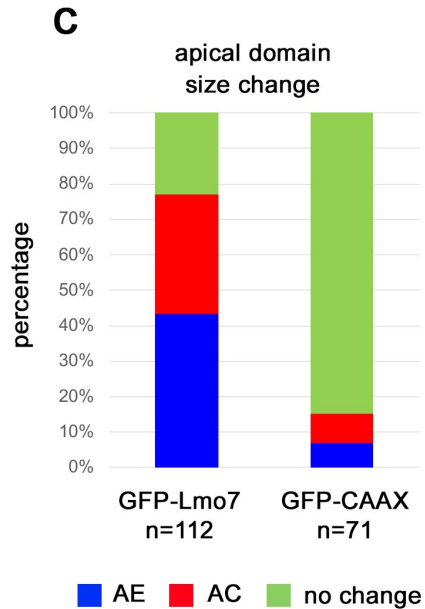
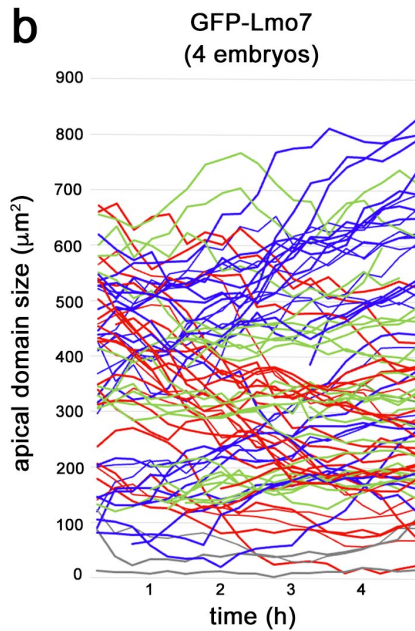
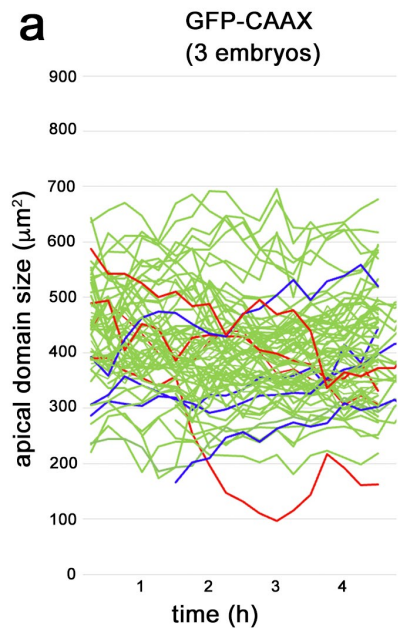
Supplementary Figure 5. Effect of the external region on cell alignment in simulations.

(a, b) Model tissue after relaxation (a) and distribution of angles between the AP axis (horizontal line) and cell elongation direction (b) at $t = 2000$ for $N'_x = 100$ and $N'_y = 34$. (c, d) Model tissue after relaxation (c) and distribution of angles between the AP axis and cell elongation direction (D) at $t = 2000$ for $N'_x = 100$ and $N'_y = 100$. (e, f) Model tissue after relaxation (e) and distribution of angles between the AP axis and cell elongation direction (f) at $t = 20000$ for $N'_x = 180$ and $N'_y = 180$. (g) Central length (along the AP axis) and width (perpendicular to the AP axis) of the model tissue, relative to those lengths at the start of the simulation, as a function of N'_y at $t = 2000$, keeping $N'_x = 100$.

a**c****b****d**

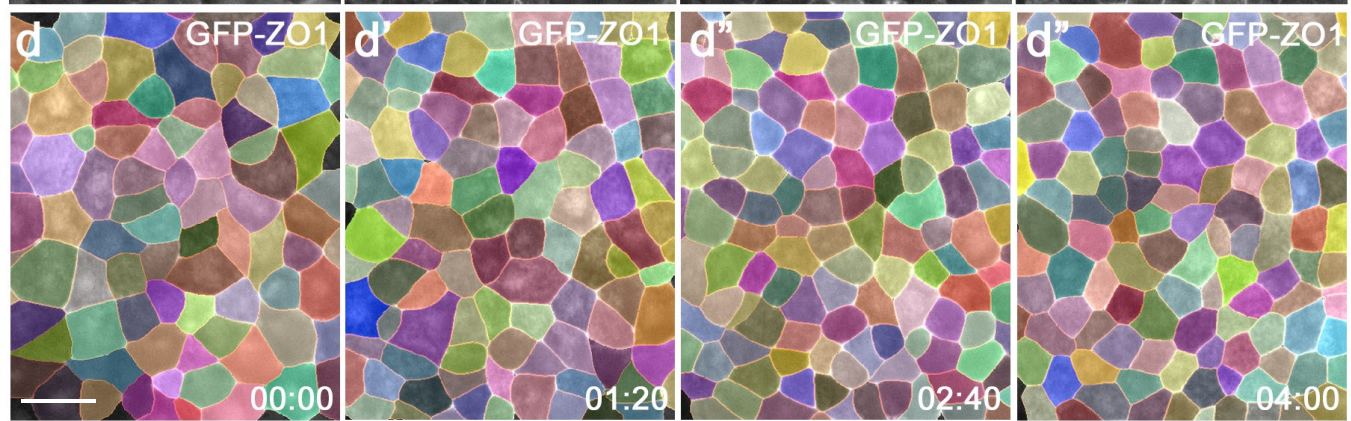
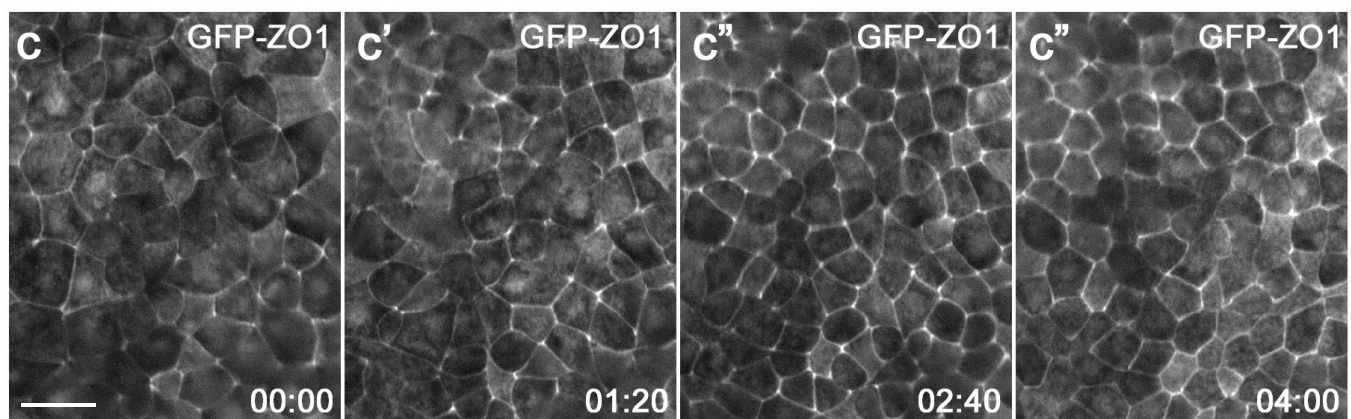
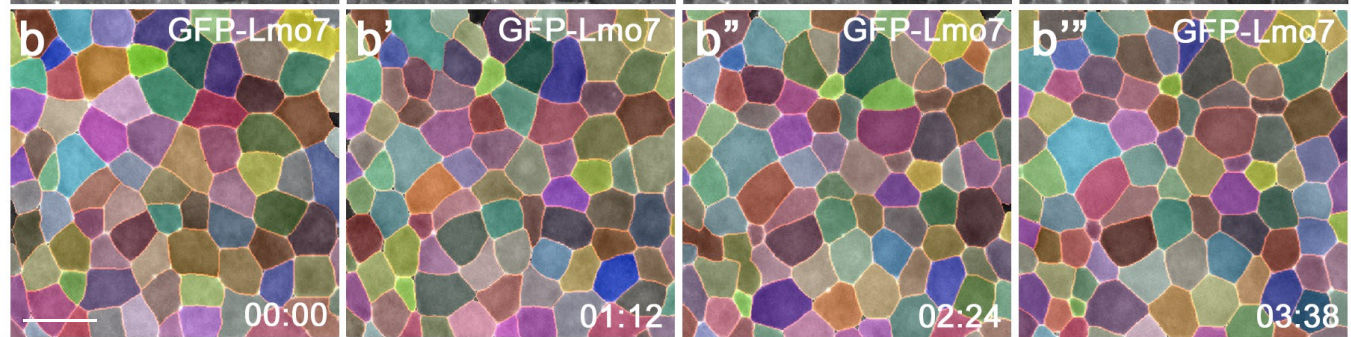
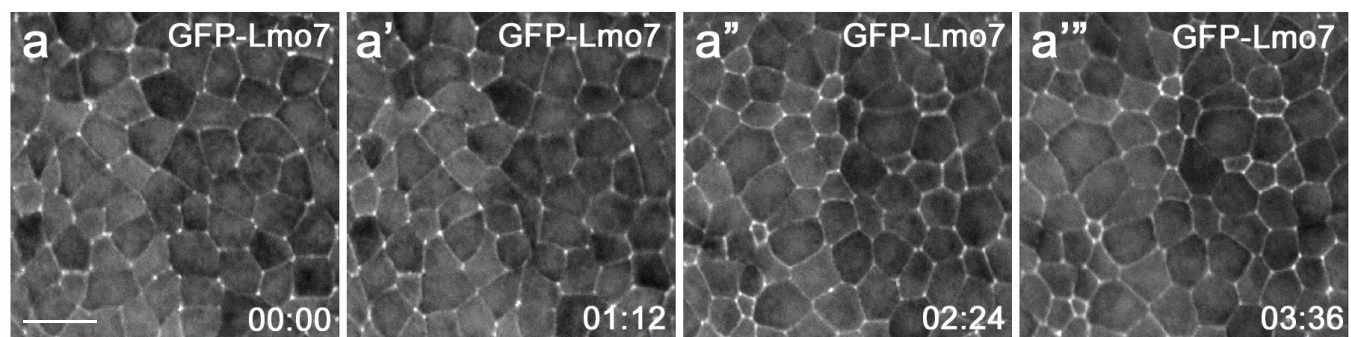
Supplementary Figure 6. Apically constricting ‘hinge cells’ contribute to neural plate cell morphology and orientation.

(a) Zoom on the neural plate region of the vertex model initial condition with separate dorsolateral hinge regions. Blue border outlines the hinges, whereas a red border outlines the region between them. Constricting cells are shown in magenta for the hinges and in cyan for the remainder of the model posterior neural plate (tissue shown for $P_h = 0.5$ and $P_c = 0.2$). (b) Model tissue from panel a after relaxation at $t = 2000$. Red lines show the direction of cell elongation. (c, d) Distribution of angles between the AP axis (horizontal line) and cell elongation direction for the model tissue in panel b for non-constricting cells in the hinges (c) and in the remainder of the neural plate (d).



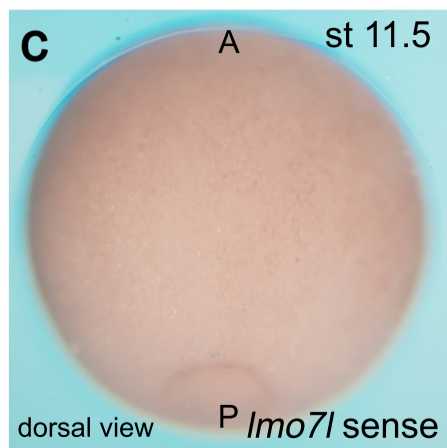
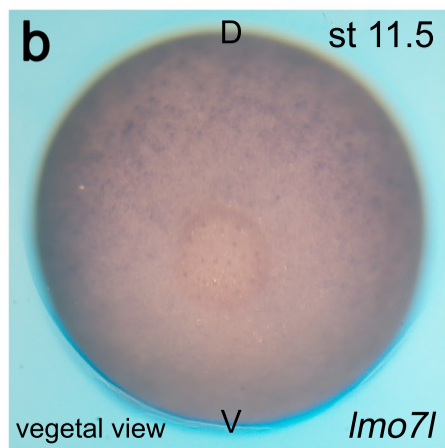
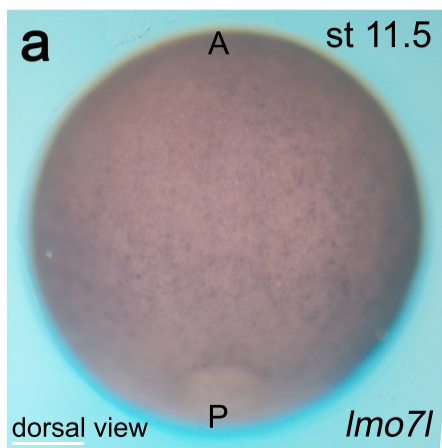
Supplementary Figure 7. Heterogeneous response of ectodermal cells to Lmo7.

(a, b) Quantification of apical domain size dynamics in GFP-CAAX (a) or GFP-Lmo7 (b) embryos. GFP-CAAX or Lmo7 RNA was injected into four animal blastomeres of 4-8-cell embryos as shown in Fig. 5a. Each line represents apical domain size change of an individual cell over 4-5 hours. AC (red) and AE (blue) cells show more than 20% decrease or increase in their apical domain size, respectively. Cells with less than 20% changes ('no change') are shown in green. Grey lines indicate cells which had the apical domain smaller than $150 \mu\text{m}^2$ at the beginning of time-lapse imaging and remained small. Data for 71 GFP-CAAX cells are from 3 embryos. Data for 112 GFP-Lmo7 cells are from 4 embryos. (c) Percentage of AC, AE and 'no change' cells in a and b. Repeated at least three times. The Freeman-Halton extension of Fisher's exact test. $p = 2.081 \text{ E-}16$.



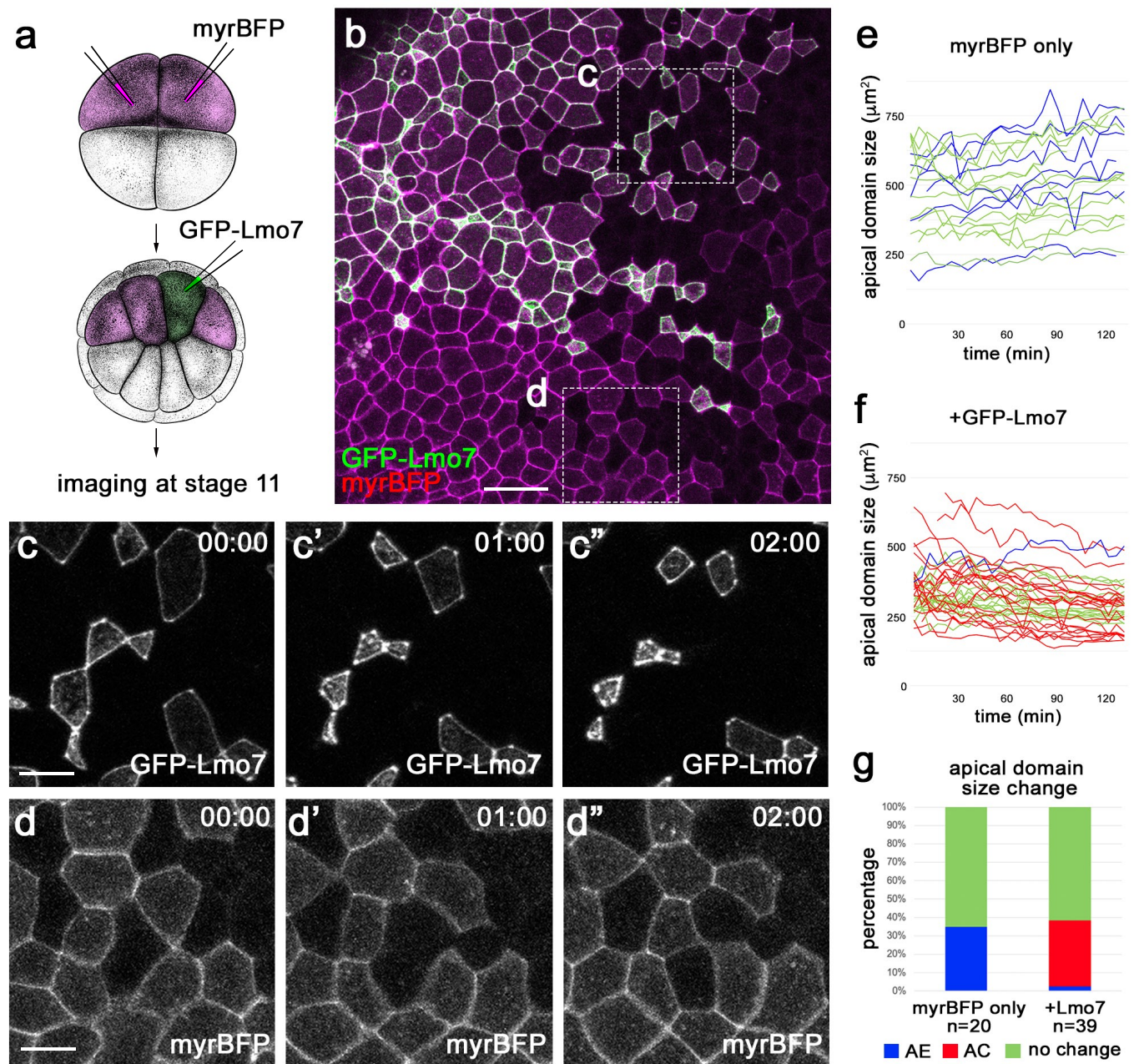
Supplementary Figure 8. Cell segmentation and cell tracking in Lmo7-expressing and control ectoderm.

Representative still images of stage 11-12 ectoderm expressing GFP-Lmo7 (a-a'') and GFP-ZO1 (c-c'') from time-lapse imaging. Segmented images of a-a'' and c-c'' are shown in b-b'' and d-d'', respectively. See Movie 2 and Movie 3. For details of segmentation and cell tracking, see Methods. Experiments were repeated at least three times. Scale bars are 40 μm .



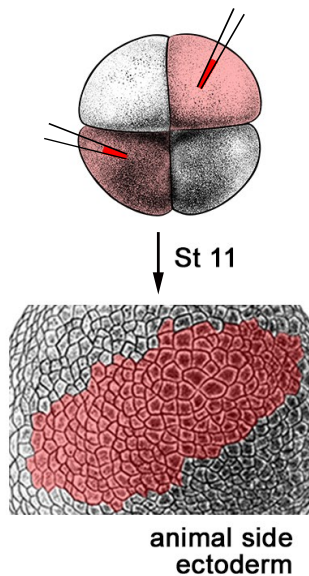
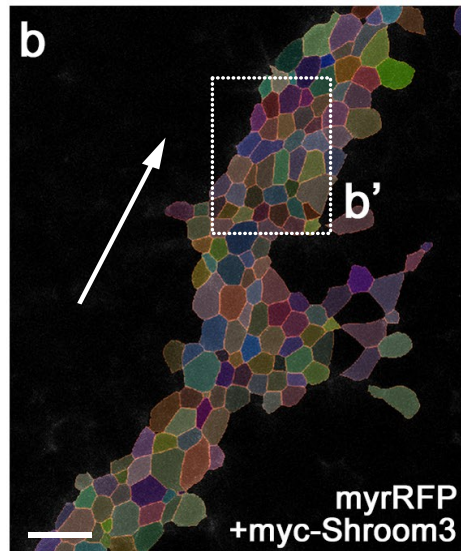
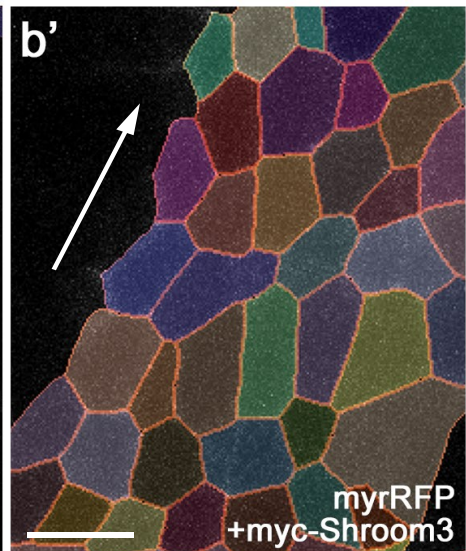
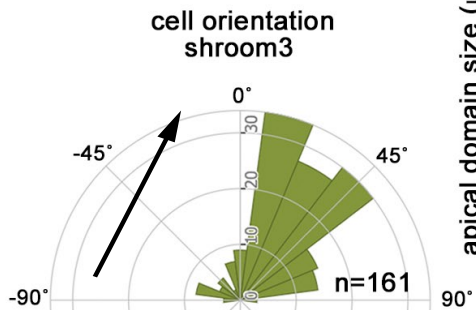
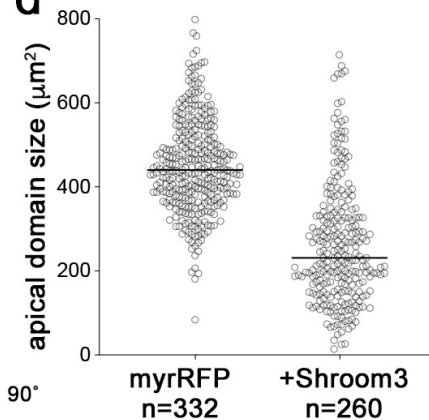
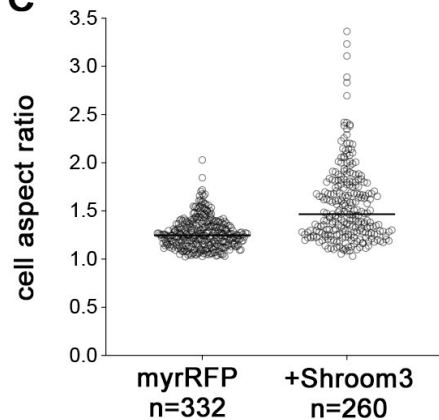
Supplementary Figure 9. Non-homogeneous distribution of *Imo7l* transcripts in late gastrulae.

Whole mount *in situ* hybridization was carried out with *Imo7l* antisense and sense probes using stage 11.5 embryos. Representative embryo images are shown. (a,b) *Imo7l* antisense probe. Dorsal view (a). Vegetal view (b). (c) *Imo7* sense probe. Dorsal view. A: anterior. P: posterior. Scale bar: 200 μ m.



Supplementary Figure 10. Apical constriction of mosaically expressing Lmo7 cells.

(a) Scheme of the experiment. myrBFP RNA (50 pg) was injected into two ventral blastomeres of 4-cell stage embryos. GFP-Lmo7 RNA (100 pg) was subsequently injected into one ventral blastomere of 16-cell stage embryos. The animal ectoderm was imaged at stage 11. Adapted from *Xenopus* illustrations © Natalya Zahn (2022), Xenbase (www.xenbase.org RRID:SCR_003280)¹. (b) Representative image of myrBFP and GFP-Lmo7 expressing embryos. (c-d”) Representative still images of GFP-Lmo7 (c-c”) and myrBFP (d-d”) cells from time-lapse imaging. (e, f) Quantification of apical domain size dynamics in myrBFP (e) and GFP-Lmo7 (f) cells. Each line represents apical domain size changes of individual cells over 2 hrs. n=20 cells for myrBFP only and n=39 for myrBFP+GFP-Lmo7 from three embryos. (g) Percentage of AC (red), AE (blue) and ‘no change’ (green) cells (See Fig. 5 legend) is shown in e and f. the Freeman-Halton extension of Fisher’s exact test. $p=0.000065$. The data represents 3-5 independent experiments.

a**b****b'****c****d****e**

Supplementary Figure 11. Shroom3 promotes apical domain heterogeneity.

(a) Scheme of the experiment for b-e. myc-Shroom3 (40 pg) and myrRFP (50 pg) RNAs were co-injected into two opposing animal blastomeres of 4-8 cell stage embryos.

Animal pole ectoderm was imaged at stage 11. Adapted from *Xenopus* illustrations © Natalya Zahn (2022), Xenbase (www.xenbase.org RRID:SCR_003280)¹. (b, b')

Representative segmented Shroom3-expressing ectoderm. Rectangular area in b is enlarged in b'. (c) Rose plot depicting cell orientation of Shroom3 cells in b and b'. n=161 cells from one embryo.

(c, e) Quantification of apical domain size (d) and cell aspect ratio (e) of myrRFP cells and myrRFP+Shroom3 cells. n=332 cells for myrRFP and n=260 cells (myrRFP+Shroom3). Two embryos each. The Kolmogorov-Smirnov test. $p < 0.000000001$ (d). $p < 0.000000001$ (e). Experiments were repeated three times.

Scale bars are 50 μm in b and 20 μm in b'.

Supplementary References

1. Zahn et al., Normal Table of Xenopus development: a new graphical resource. *Development* (2022) 149 (14): dev200356. <https://doi.org/10.1242/dev.200356>